

1. MOTIVATION

The lunar surface consists of a regolith layer, i.e., fragmental and unconsolidated rock material of highly varied character, which covers the underlying bedrock. Understanding the structure, composition, and dynamics of the lunar regolith and the underlying bedrock is very important to reveal geologic features of the Moon, explore natural resources humans can exploit, and obtain valuable information regarding the history of the solar system.

Electromagnetic radiations from the surface of the Moon at microwave frequencies depend on the physical, chemical, and thermal properties of the regolith layer and the bedrock. Moreover, the electromagnetic penetration depth changes with frequency which may allow wideband microwave radiometers operating below 50 GHz to conveniently profile these properties versus depth to characterize the lunar regolith and bedrock with wide spatial coverage.

2. PHYSICAL AND ELECTRICAL PROPERTIES OF LUNAR REGOLITH

Regolith Density

$$\rho(z) = 1.92 \frac{z - 12.2}{z + 18}$$

where ρ is the bulk density in g/cm^3 and z is the depth in cm [1].

Regolith Physical Temperature

$$T(z, t) = T_o + \Delta T_o e^{-z/\sqrt{2\alpha}} \sin\left(\omega t - z\sqrt{\omega/2\alpha}\right)$$

where z and t are the depth and time, T_o is the mean surface temperature, ΔT_o and ω are the surface temperature fluctuation amplitude and frequency, and α is the thermal diffusivity [2].

Electrical Properties of the Regolith

$$\epsilon'(z) \approx 10^{0.27\rho(z)}$$

$$\epsilon''(f, z) \approx \epsilon'(z) \times 10^{(0.0272f + 0.2967)\rho(z) + 0.027p_{ch} - 3.058}$$

where f is frequency in GHz and p_{ch} is the percentage of TiO_2 and FeO amount [3-4]. Using these models, and assuming the electromagnetic scattering is negligible in the regolith, we can approximately compute the normal incidence brightness temperatures at the regolith surface, $T_{BS} = T_B(z = 0, f)$, as:

$$T_{BS} = (1 - R_{air-reg}) \times \left[\int_{z_{base}}^{z=0} \alpha(f, z) T(z) e^{-\int_{z'=z}^{z'=0} \alpha(z', f) dz'} dz + (1 - R_{reg-base}) T_{base} e^{-\int_{z_{base}}^{z=0} \alpha(z, f) dz} \right]$$

where $R_{air-reg}$ is the amplitude squared of the Fresnel reflection coefficient at the air-regolith boundary, $T(z)$ is the physical regolith temperature at depth z , $R_{reg-base}$ is the amplitude squared of the Fresnel reflection coefficient at the bedrock-regolith boundary, T_{base} is the physical temperature of the bedrock, and

$$\alpha(f, z) = -1 \times \text{imag} \left\{ 2\pi f \sqrt{\mu_0 \epsilon_0} (\epsilon'(z) - i\epsilon''(f, z)) \right\}$$

is the electromagnetic attenuation coefficient in the regolith.

3. CHANG'E-1 AND CHANG'E-2 MISSIONS

Chang'E-1 and Chang'E-2 missions of the Chinese Lunar Exploration Program measured brightness temperatures of lunar surfaces via their nadir-looking microwave radiometers between 2007-2009 and 2010-2011, respectively. The measurements were done with four frequency channels at 3 GHz, 7.8 GHz, 19.35 GHz, and 37 GHz. Spatial resolution of the measurements were 50-35 km for Chang'E-1 and 25-17.5 km for Chang'E-2 due to different altitudes of the instruments.

4. SIMULATED VS MEASURED BRIGHTNESS TEMPERATURES

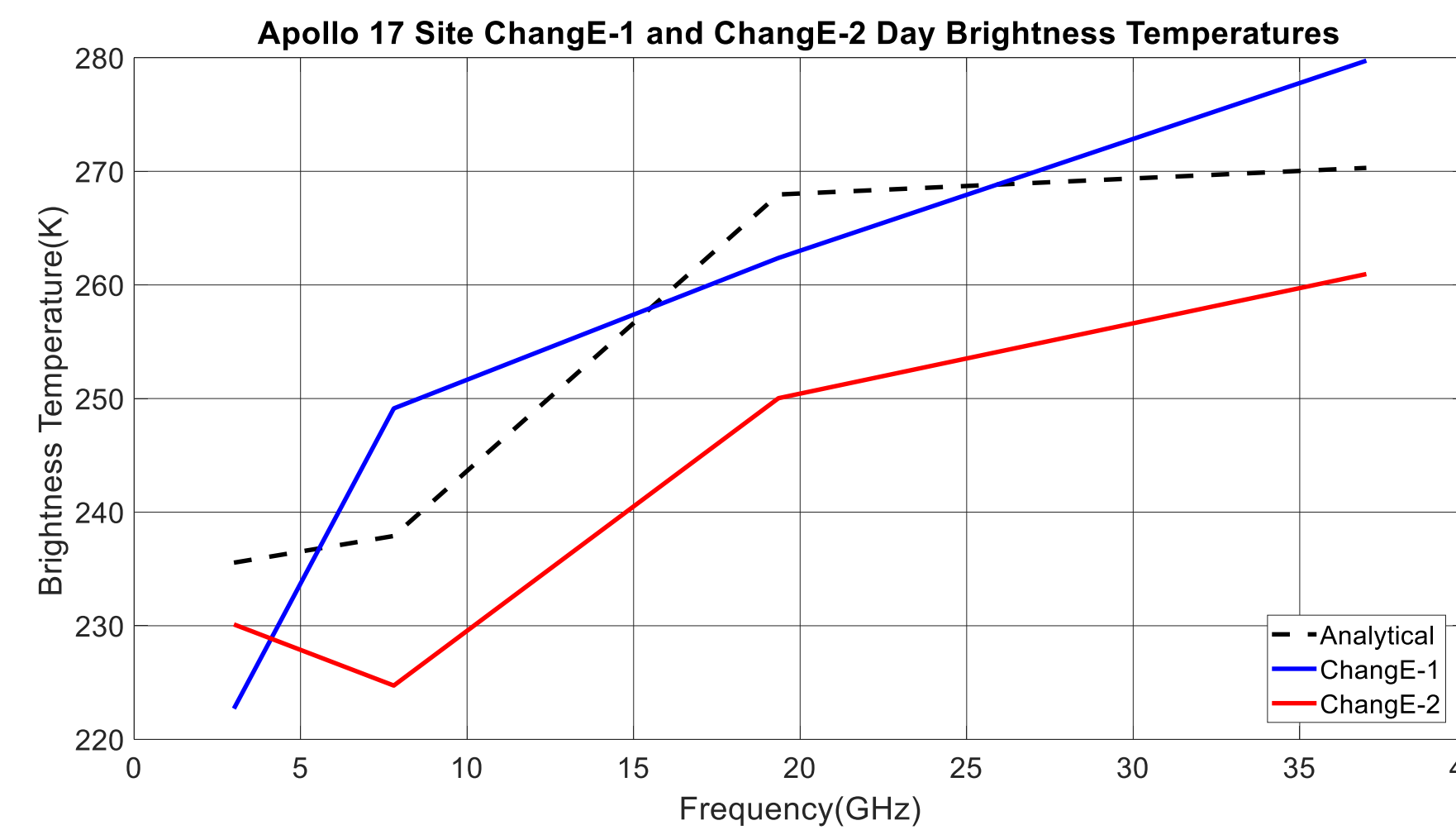


Figure 3. Average surface brightness temperatures measured by Chang'E-1 and Chang'E-2 over the Apollo 17 site during lunar days compared with the analytical calculations. Although the trends are similar, the differences between measured and simulated brightness temperatures can be as large as 20 K.

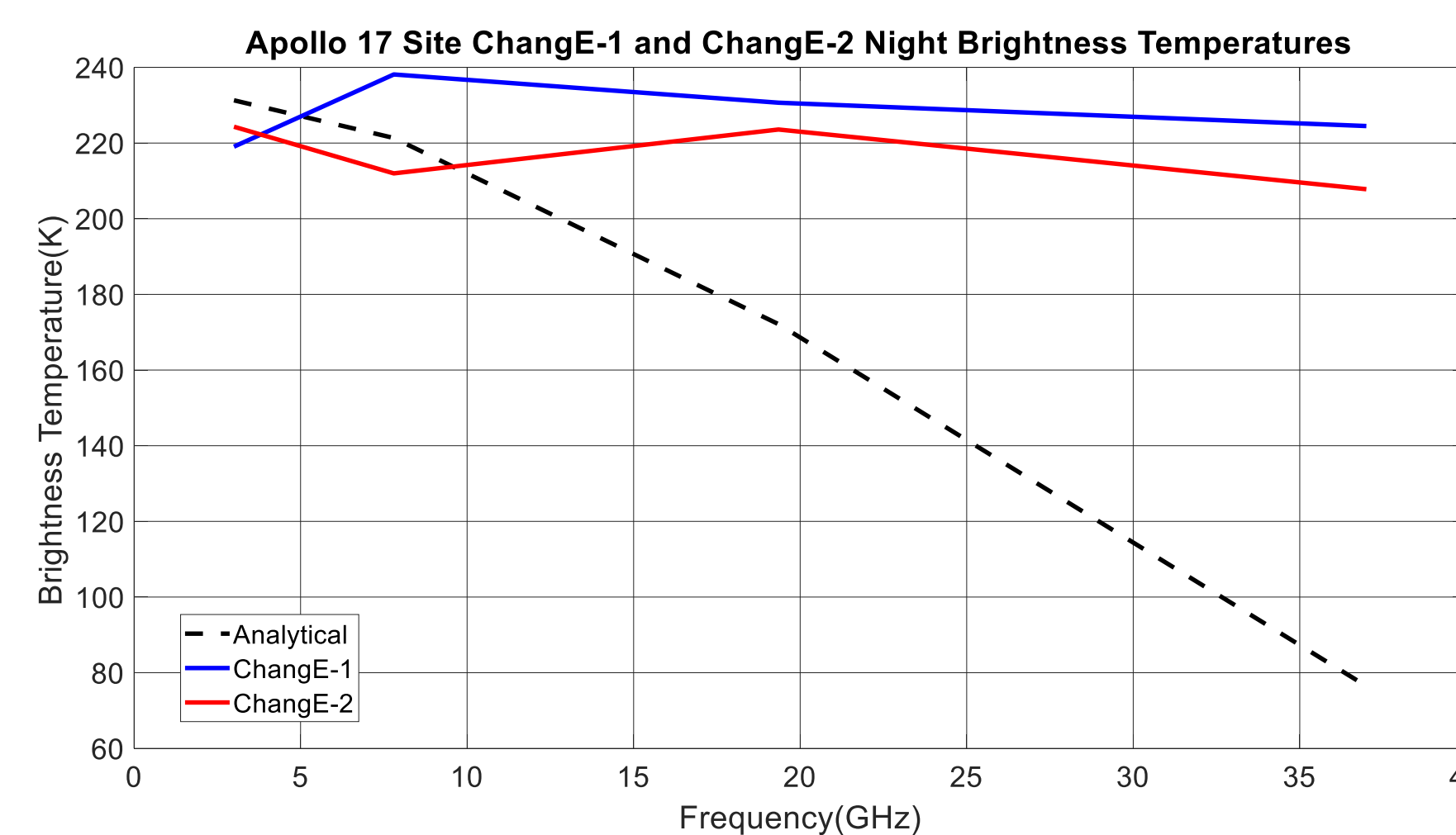


Figure 4. Average surface brightness temperatures measured by Chang'E-1 and Chang'E-2 over the Apollo 17 site during lunar nights compared with the analytical calculations. Simulated brightness temperatures are found to be much lower than the actual measurements at high frequencies which requires further investigations.

Electrical properties, i.e., complex permittivity, of the lunar regolith should be characterized over a wide range of temperatures and frequencies in the microwave spectrum with special emphasis on cold temperatures and high frequencies.

More comprehensive forward emission models are needed for accurate brightness temperature simulations.

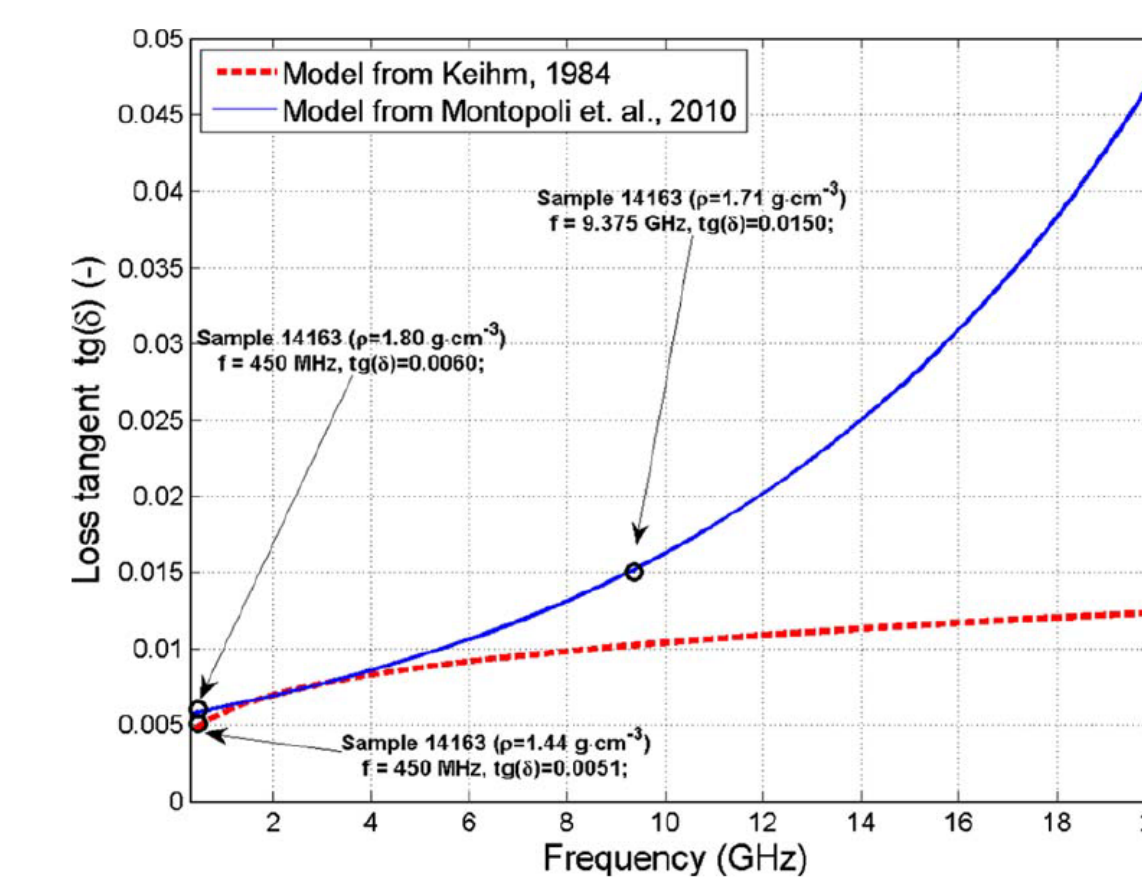


Figure 5. Electromagnetic loss tangent models for lunar regolith [4].

5. IMPORTANT OBSERVATIONS

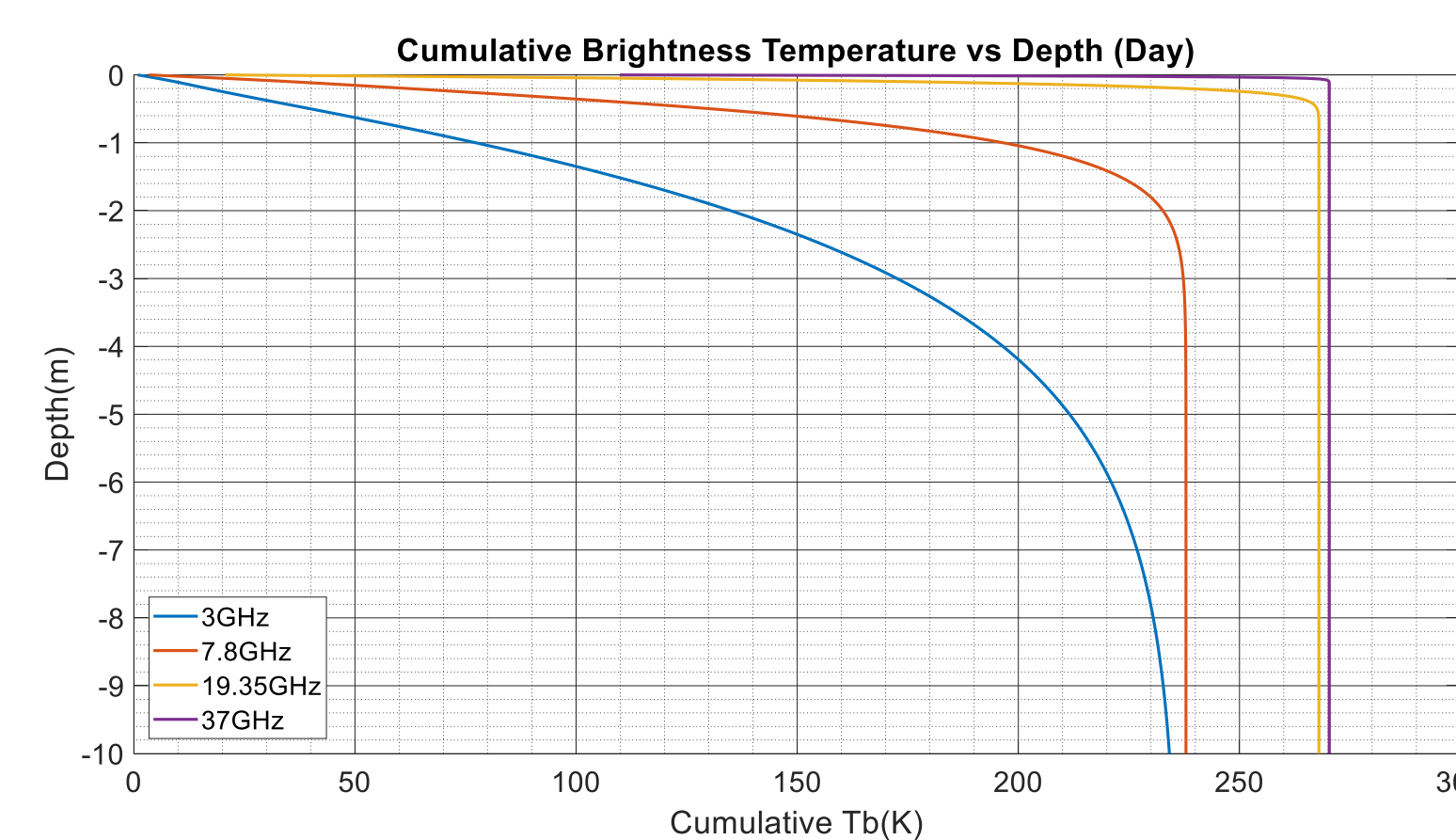


Figure 6. Cumulative brightness temperatures found by summing emissions from the surface to each depth at Chang'E-1 and Chang'E-2 frequencies. Notice that as frequency increases contributions from the deeper layers decreases. Higher frequencies are sensitive to only very shallow regolith.

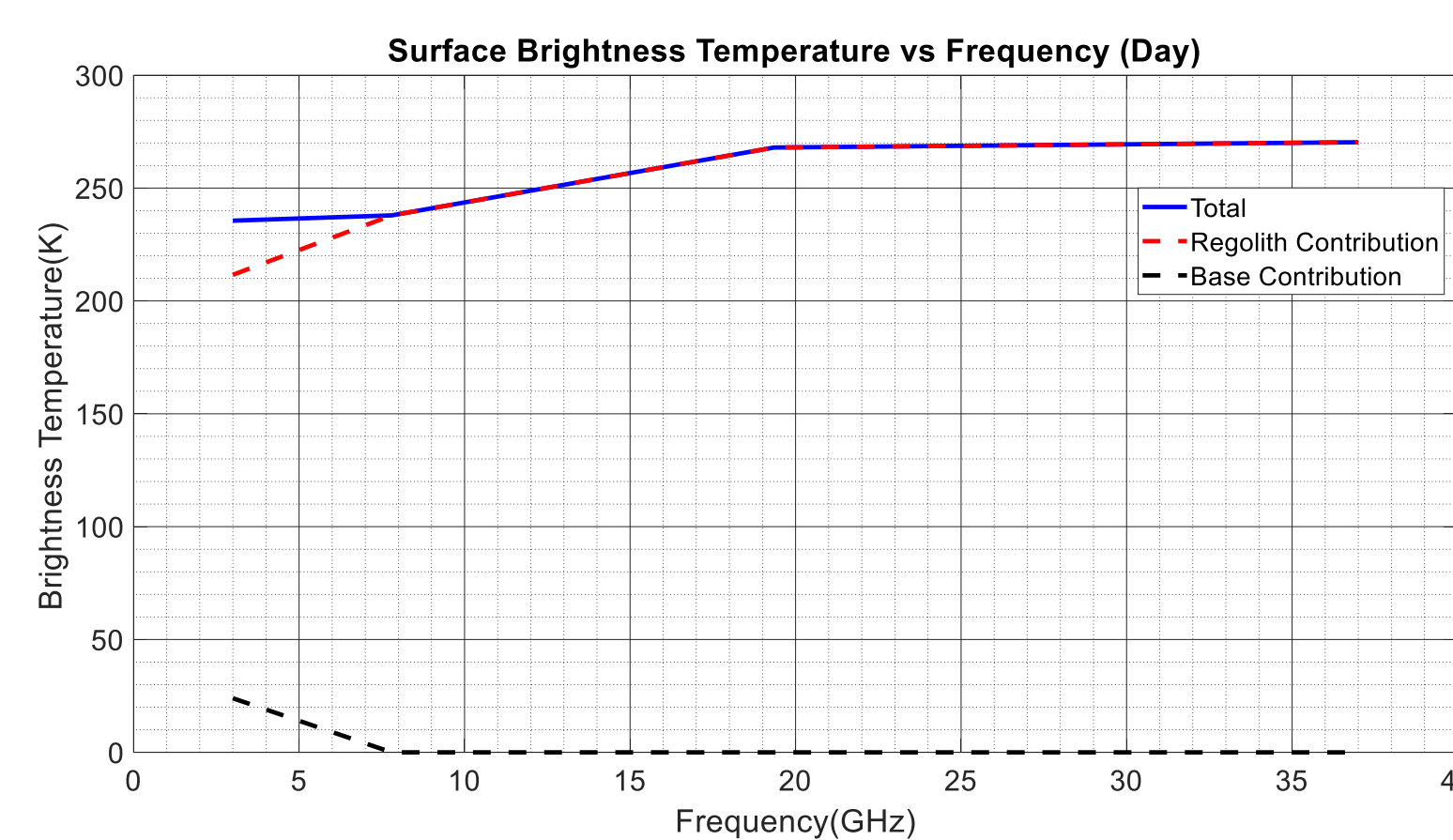


Figure 7. Surface brightness temperatures at Chang'E-1 and Chang'E-2 frequencies for a 5-meter regolith with rock base. Notice that brightness temperatures at low frequencies may be sensitive to the bedrock.

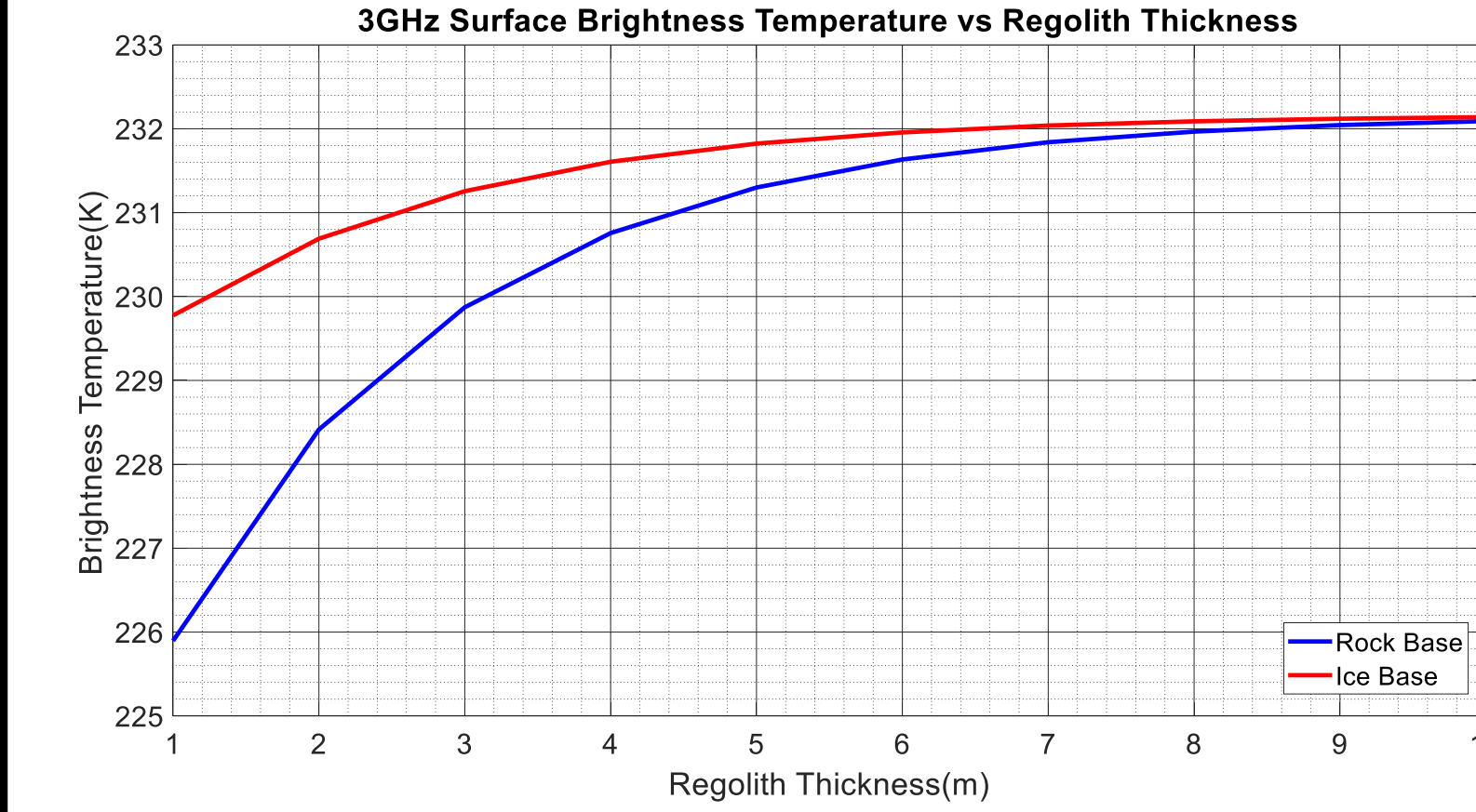


Figure 8. 3 GHz surface brightness temperatures computed for regolith on rock and ice bases versus the regolith thickness. Notice the significant impact of the bedrock type on surface brightness temperatures for thinner regolith.

Preliminary analyses have demonstrated that thermal, physical, and chemical properties of the lunar regolith and bedrock can be profiled versus depth via wideband microwave radiometry utilizing the considerable change in the electromagnetic penetration depth across the microwave spectrum.

However, first, more comprehensive forward microwave emission models should be developed to include volume scatterings, roughness of bedrock and regolith layers, density fluctuations within the regolith, coherent wave interferences, and temperature dependency of the regolith permittivity etc.

6. FUTURE WORK

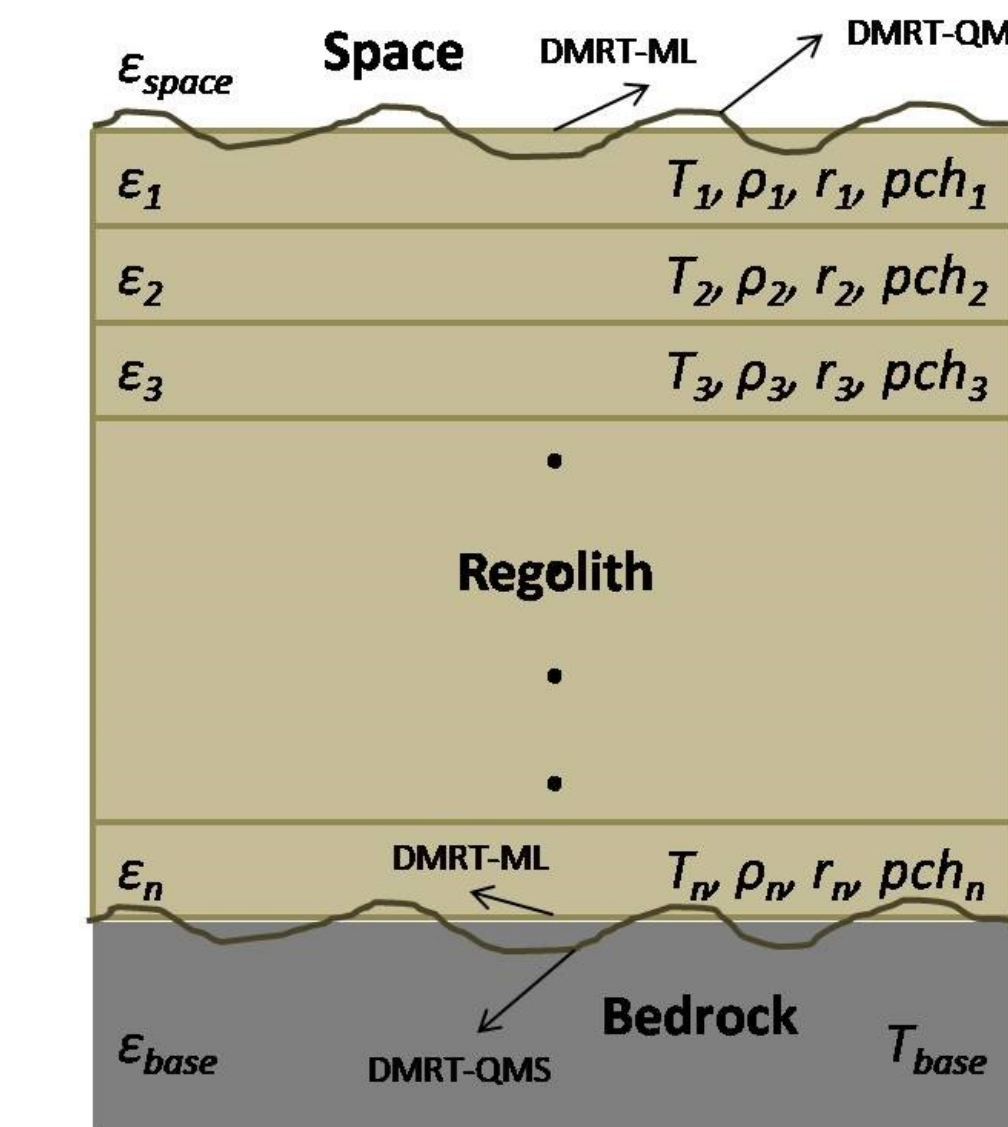


Figure 9. DMRT-ML and DMRT-QMS for lunar studies

DMRT-ML and DMRT-QMS models (developed in Fortran and MATLAB, respectively and available to public) can be modified for lunar studies and used as more accurate forward microwave emission models for lunar regolith and bedrock.

Once a reliable forward emission model is established, numerical retrieval algorithms can be developed to retrieve the physical, thermal, and chemical properties of the lunar regolith and bedrock versus depth.



Figure 10. Recent developments in radiometer design and CubeSat technologies may enable future lunar missions which carry wideband microwave radiometers for passive remote sensing of lunar regolith and bedrock. The figure demonstrates the CubeRRT (CubeSat Radiometer RFI Technology Validation) instrument which carries a microwave radiometer operating in the 6-40 GHz band [7].

7. REFERENCES

- [1] Chen, Ping, et al. "Effects of slightly rough surfaces on the brightness temperature of the lunar regolith." *Radio Science* 48.3 (2013): 265-273.
- [2] Aschwanden, Andy. "Thermodynamics of Glaciers." (2010).
- [3] Montopoli, Mario, et al. "Remote sensing of the Moon's subsurface with multifrequency microwave radiometers: A numerical study." *Radio Science* 46.1 (2011).
- [4] Montopoli, Mario, et al. "Lunar microwave brightness temperature: Model interpretation and inversion of spaceborne multifrequency observations by a neural network approach." *IEEE Transactions on Geoscience and Remote Sensing* 49.9 (2011): 3350-3358.
- [5] Picard, G., et al. "Simulation of the microwave emission of multi-layered snowpacks using the Dense Media Radiative transfer theory: the DMRT-ML model." (2013). <http://pp.ige-grenoble.fr/pageperso/picardgh/dmrtml/>
- [6] Tsang, Leung., et al. "DMRT-QMS (QCA Mie scattering of Sticky spheres) v0.1." Remote Sensing Code Library (RSCL) January, 2018 Newsletter. <http://web.eecs.umich.edu/~leutsang/Computer Codes and Simulations.html>
- [7] "CubeRRT." Gunter's Space Page. space.skyrocket.de/doc_sdat/cubertrt.htm.